



Change Detection in Satellite Images using Reconstruction Errors of Joint Autoencoders

Ekaterina Kalinicheva, Jeremie Sublime, Maria Trocan

► To cite this version:

Ekaterina Kalinicheva, Jeremie Sublime, Maria Trocan. Change Detection in Satellite Images using Reconstruction Errors of Joint Autoencoders. Artificial Neural Networks and Machine Learning – ICANN 2019: Image Processing, pp.637-648, 2019, 10.1007/978-3-030-30508-6_50 . hal-02559342

HAL Id: hal-02559342

<https://hal.archives-ouvertes.fr/hal-02559342>

Submitted on 30 Apr 2020

HAL is a multi-disciplinary open access archive for the deposit and dissemination of scientific research documents, whether they are published or not. The documents may come from teaching and research institutions in France or abroad, or from public or private research centers.

L'archive ouverte pluridisciplinaire **HAL**, est destinée au dépôt et à la diffusion de documents scientifiques de niveau recherche, publiés ou non, émanant des établissements d'enseignement et de recherche français ou étrangers, des laboratoires publics ou privés.

Change Detection in Satellite Images using Reconstruction Errors of Joint Autoencoders

Ekaterina Kalinicheva¹, Jérémie Sublime^{1,2}, and Maria Trocan¹

¹ LISITE - DASSIP Team

ISEP, 10 rue de Vanves, 92130 Issy-Les-Moulineaux, France

`firstname.lastname@isep.fr`

² LIPN - CNRS UMR 7030

99 av. J-B Clément, 93430 Villetaneuse, France

`firstname.lastname@lipn.univ-paris13.fr`

Abstract. With the growing number of open source satellite image time series, such as SPOT or Sentinel-2, the number of potential change detection applications is increasing every year. However, due to the image quality and resolution, the change detection process is a challenge nowadays. In this work, we propose an approach that uses the reconstruction losses of joint autoencoders to detect non-trivial changes (permanent changes and seasonal changes that do not follow common tendency) between two co-registered images in a satellite image time series. The autoencoder aims to learn a transformation model that reconstructs one co-registered image from another. Since trivial changes such as changes in luminosity or seasonal changes between two dates have a tendency to repeat in different areas of the image, their transformation model can be easily learned. However, non-trivial changes tend to be unique and can not be correctly translated from one date to another, hence an elevated reconstruction error where there is change. In this work, we compare two models in order to find the most performing one. The proposed approach is completely unsupervised and gives promising results for an open source time series when compared with other concurrent methods.

Keywords: satellite images · change detection · autoencoder · unsupervised learning · reconstruction loss.

1 Introduction

Nowadays, change detection in satellite image time series (SITS) is required for many different applications. Among them, there are numerous ecological applications such as the analysis and preservation of the stability of ecosystems or the detection and the analysis of phenomena such as deforestation and droughts, the studies of economical development of cities, the analysis of vegetation state for different agricultural purposes, etc. While in some applications, we are interested in seasonal changes such as evolutions in agricultural parcels, others require the detection of the permanent changes such as buildings or roads constructions. Nevertheless, due to image resolution and preprocessing level (most of the SITS

do not have a correction of the atmospheric factors), properly detecting changes remains a difficult task.

Different algorithms for change detection are proposed in the literature. For example, in [5] the authors use PCA and hybrid classification methods for change detection in urban areas. The authors of [2] propose siamese neural networks for supervised change detection in open source multispectral images.

However, most change detection algorithms are supervised or semi-supervised, and therefore need some labeled data. Providing the labeled data for remote sensing images and especially SITS is a costly and time-consuming task due to the variance of objects present in them and the time needed to produce the large amount of labeled images required to train large models.

This lack of labeled data and the difficulty to acquire them is not specific to SITS and remains true for any application with satellite images. This issue has encouraged the use of unsupervised methods to tackle this type of images especially, when the number of features is large or when the images are very complex [12].

In this paper, we propose an unsupervised approach based on a neural network autoencoder (AE) algorithm for non-trivial change detection in SITS. The algorithm is based on change detection between two bi-temporal images Im_n and Im_{n+1} . Needless to say, it can be also applied to two co-registered images instead of a SITS. In the presented approach, we use joint AEs to create models able to reconstruct Im_{n+1} from Im_n and vice versa by learning the image features. Obviously, the non-changed areas and trivial changes such as seasonal ones will be easily learned by the model, and therefore reconstructed with small errors. As the non-trivial changes are unique, they will be considered as outliers by the model, and thus will have a high reconstruction error (RE). Thresholding on the RE values allows us to create a binary change map (CM). The proposed method has showed promising results on a dataset with high ratio of agricultural areas and outperformed the concurrent approach. Different joint AE models were tested in order to find the most accurate. Our method has a low complexity and gives high quality results on open source high resolution (HR) images.

The remainder of this article is organized as follows: In section 2, we present related works. Section 3 details our proposed approach. Section 4 is dedicated to experimental results and some conclusions and future work perspectives are drawn in section 5.

2 Related works

The main difficulty with unsupervised approaches to analyze satellite images is that they usually produce lower quality results than supervised ones. To improve the quality of unsupervised change detection between two images, the fusion of results from different algorithms is often proposed [6]. At the same time, automatic methods for selection of changed and unchanged pixels are used to obtain training samples for a multiple classifier system [13]. Following this paper, the authors of [1] propose the improved backpropagation method of a deep belief

network (DBN) for change detection based on automatically selected change labels.

Nevertheless, classic feature comparison approaches do not separate trivial (seasonal) changes from non-trivial ones (permanent changes and changes that do not follow seasonal tendency). This weakness can drastically complicate the interpretation of change detection results for regions with high ratio of vegetation areas. In fact, when analyzing two images belonging to different seasons of the year, almost all the area will be marked as change and further analysis will be needed to identify meaningful changes (non-trivial).

In [10], a regularized iteratively reweighted multivariate alteration detection (MAD) method for the detection of non-trivial changes was proposed. This method is based on linear transformations between different bands of hyperspectral satellite images and canonical correlation analysis. However, spectral transformation between multi-temporal bands is very complex. For these reasons, deep learning algorithms which are known to be able to model non-linear transformations have proved their efficiency to solve this problem [14].

Our method is based on the approach proposed in [14]. In this work, the authors use a Restricted-Boltzmann Machines-based (RBM) model to learn the transformation model for a couple of very high resolution (VHR) co-registered images Im_1 and Im_2 . RBM is a type of stochastic artificial network that learns the distribution of the binary input data. When dealing with the continuous data, Gaussian-Bernoulli RBM (GBRBm) is used [9].

The principle of the proposed method to detect changes is the following: most of the trivial changes can be easily modeled from Im_1 to Im_2 , at the same time, non-trivial changes will not be properly reconstructed. Therefore, the reconstruction accuracy can be used to detect the non-trivial change areas.

The proposed approach consist of the following steps: feature learning, feature comparison and thresholding. During the feature learning step, the algorithm learns some meaningful features to perform transformation of patches of Im_1 to the patches of Im_2 . Once the features are learned by the model, Im_1 is transformed in Im'_2 . Then the difference image (DI) of Im_2 and Im'_2 is calculated. The same steps are performed to create a DI of Im_1 and Im'_1 . The thresholding is then applied on an average DI. Obviously, the areas with high difference values will be the change areas.

For the feature learning, the authors use an AE model composed of stacked RBMs layers GBRBM1-RBM1-RBM2-GBRBm2. The authors indicate that the algorithm is sensitive to changing luminosity and has high level of false positive changes in real change data. To our knowledge, the algorithm was tested only on urban areas.

3 Proposed approach

Our method is similar with the one presented in [14] that we have introduced in the previous section. However, contrary to RBM models that are based on a stochastic approach and distribution learning, we propose to use a deterministic

model based on feature extraction. Furthermore, we use patch reconstruction error for every pixel of the image - instead of image difference - as extracting features from every pixel neighborhood is an important step for any eventual subsequent pixel-wise classification task.

Classical AEs are a type of neural network where the input is the same as the output. During the learning process, the encoding pass of the model learn some meaningful representation of the initial data that is being transformed back during the decoding pass. In our work, we test two deterministic AE architectures and assess their performance for change detection in order to pick the best adapted one. The tested models are joint fully-convolutional AEs and joint convolutional AEs.

Fully-convolutional AEs consist of a stack of layers that apply different convolutions (filters) to the input data in order to extract meaningful feature maps (FM) (Figure 1). Convolutions are often used in image processing as they deal with non-flattened data (2D and 3D). Therefore, unsupervised feature extraction with fully-convolutional AEs has been proved efficient in different remote sensing applications [4]. Convolutional AEs equally contain different convolutional layers that are followed by some fully-connected layers to compress the feature maps. Usually these AEs are used for image clustering as FC layers perform the dimensionality reduction [8].

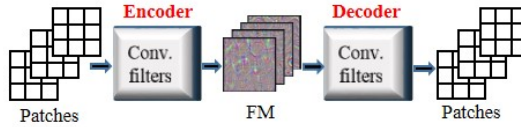


Fig. 1. Fully-convolutional AE model. Pre-training phase.

3.1 Change detection algorithm

Let $Im_1, Im_2, \dots, Im_{S-1}, Im_S$ be a SITS made of S co-registered images taken at dates $T_1, T_2, \dots, T_{S-1}, T_S$. Our algorithm steps are the followings, see Figure 2:

- The preprocessing step consists of a relative radiometrical normalization [7]. It reduces a number of potential false and missed change alarms related to the changing luminosity of objects.
- The first step of change detection algorithm consist in model pre-training on the whole dataset (Figure 2).
- During the second step, we fine-tune the joint AE model for every couple of images (Im_n, Im_{n+1}). Once the model is trained, we calculate the reconstruction error of Im'_{n+1} from Im_n and vice versa for every patch of the images. In other words, the reconstruction error of every patch is associated to the position of its central pixel on the image.

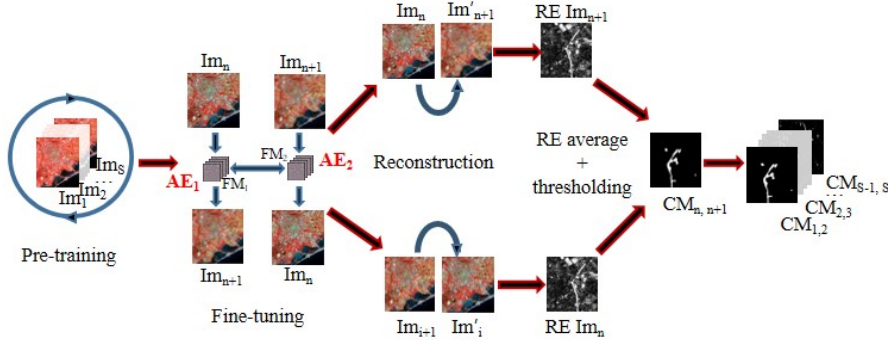


Fig. 2. Change detection algorithm.

- In the last step, we identify areas of high reconstruction error using Otsu’s thresholding method [11] in order to create a binary change map $CM_{n,n+1}$ with non-trivial change areas.

3.2 Model pre-training and fine-tuning

In our method, we use deep AEs to reconstruct Im_{i+1} from Im_i . During the model pre-training, the feature learning is performed patch-wise for a sample extracted from the SITS. In our method, we sample $\frac{H \times W}{S}$ patches (H and W represent image height and width, respectively) from every image to prevent the model from overfitting. The patches for the border pixels are generated by mirroring the existing ones in the neighborhood. During the encoding pass, the model extracts feature maps (FM) for the fully-convolutional AE (and feature vector for the convolutional AE) of i, j, m -patch of chosen samples, and then during the decoding pass, it reconstructs them back to the initial i, j, m -patch ($i \in [1, H], j \in [1, W], m \in [1, S]$).

The fine-tuning part consists of learning two joint reconstruction models AE_1 and AE_2 for every patch of a couple of co-registered images (Im_n, Im_{n+1}). The patches are extracted, for every pixel of the images ($H \times W$ patches in total) as the local neighborhood wherein the processed pixel is the central one (i.e., the image i, j -pixel corresponds to i, j -patch central pixel).

Our joint fully-convolutional AEs model is presented in Figure 2). The joint model for the convolutional AE has the same structure. AE_1 and AE_2 have the same configuration of layers as the pre-trained model, and are initialized with the parameters it learned. In the joint model, AE_1 aims to reconstruct patches of Im'_{n+1} from patches of Im_n and AE_2 reconstructs Im'_n from Im_{n+1} . The whole model is trained to minimize the difference between: the decoded output of AE_1 and Im_{n+1} , the decoded output of AE_2 and Im_n , and the encoded outputs of AE_1 and AE_2 .

In our work, we use the mean squared error (MSE) for model optimization and calculation of the patch reconstruction error.

Once the model is trained and stabilized, we perform the image reconstruction of Im'_n and Im'_{n+1} for every patch, and we create two images representing their reconstruction errors. We apply Otsu's thresholding [11] to the average reconstruction error of these images in order to produce a binary change map.

4 Experimental results

4.1 Dataset

Our algorithm was applied to a SPOT-5 SITS of Montpellier area, France, taken between 2002 and 2008. This SITS belongs to the archive Spot World Heritage³. This particular SITS was chosen due to its high ratio of agricultural zones and progressive construction of new areas. The preprocessing level of SITS is 1C (orthorectified images, reflectance of the top of atmosphere). We kept only green, red and NIR bands that have 10 meters resolution as they are the most pertinent. The original images are clipped to rectangular shapes of 1600×1700 pixels, radiometrically normalized and transformed to UTM zone 31N: EPSG Projection (transformation from geographic coordinate system in degree coordinates to a projected coordinate system in meter coordinates).

4.2 Results

As mentioned in section 3, we propose different architectures: convolutional and joint fully-convolutional AEs, and we compare them in order to assess their strengths and weaknesses. We further compare our approaches with the RBM-based method presented in [14] that we have discussed in section 2 and with improved RBM method. Initially, in [14] the images are clipped in $\frac{H \times W}{p \times p}$ not overlapped patches. In the improved method, we propose to extract patches with neighborhoods of every pixel of the image ($H \times W$ patches). Equally, we use the patch reconstruction error instead of the image difference to detect the changes. In other words, the improved RBM method uses the same steps as in our proposed algorithms.

In the experiments, we use the architectures presented in Table 1, where B is the number of spectral bands and p is the patch size (in these reported results, the patch size is 5×5 for all our methods, the patch size is justified later in text). The following parameters were chosen for all convolutional layers: kernel size=3, stride=1, padding=1. Adam algorithm was used to optimize the models. During the pre-training phase, the learning rate was set to 0.0005 and then changed to 0.00005 for the fine-tuning phase.

The RBM model presented in [14] is developed for VHR images, but we have kept the patch size 10×10 pixels and the layer sizes suggested by the authors. In the improved RBM method we use 5×5 pixels patch size as in our methods.

³ Available on www.theia-landsat.cnes.fr

Table 1. Models architecture.

	F-conv.AE	Conv.AE	RBM	Impr. RBM
encoder	C(B,32)+R	C(32,32)+R	GBRBm($p^2 \times B, 384$)+S	GBRBm($p^2 \times B, (p+1)^2 \times B$)+S
	C(32,32)+R	C(32,64)+R		RBM(($p+1$) $^2 \times B, (p-2)^2 \times B$)+S
	C(32,64)+R	C(64,64)+R	RBM(384,150)+S	GBRBm($(p+1)^2 \times B, (p-2)^2 \times B$)+S
	C(64,64)+ ℓ_2	L($64 \times p^2, 12 \times p^2$)+R L($12 \times p^2, 2 \times p^2$)+ ℓ_2		
decoder	C(64,64)+R	L($2 \times p^2, 12 \times p^2$)+R	RBM(150,384)+S	RBM(($p-2$) $^2 \times B, (p+1)^2 \times B$)+S
	C(64,32)+R	L($12 \times p^2, 64 \times p^2$)+R		GBRBm($(p+1)^2 \times B, p^2 \times B$)+S
	C(32,32)+R	C(64,32)+R	GBRBm($384, p^2 \times B$)+S	
	C(32,B)+S	C(32,32)+R C(32,B)+S		

C- Convolutional, L- Linear, R- ReLU, S- Sigmoid, ℓ_2 - ℓ_2 -norm

We apply ReLU and sigmoid activation functions as well as ℓ_2 -normalization to the different layers outputs.

In our approaches and in improved RBM method, before learning the Otsu's threshold, we exclude 0.5% of the highest values under the hypothesis that they correspond to some noise and extreme outliers.

We assess the algorithms performances on two extracts from the SPOT-5 SITS. The image couples were taken between May 2004 and April 2005 for the first extract, and between February 2006 and August 2008 for the second one. To evaluate the proposed approaches, we compare the obtained results with ground truth change maps. These ground truths were created for an extract of the image of size 800×600 pixels (48 km^2) for the first couple and for 320×270 pixels ($8,64 \text{ km}^2$) for the second one. However, the change detection was performed on the full images of 1600×1700 pixels (272 km^2).

The following quality criteria were used to evaluate the performances of the different approaches: precision (1), recall (2) and Cohen's kappa score [3].

$$Precision = \frac{TruePositives}{TruePositives + FalsePositives} \quad (1)$$

$$Recall = \frac{TruePositives}{TruePositives + FalseNegatives} \quad (2)$$

The patch size of 5×5 pixels was chosen empirically, however, the correlation between the patch size and the performance of our algorithms is shown in Table 2. We can observe that $p = 3$ gives us poor results for both methods as the patch do not contain enough information about the neighborhood, $p = 7$ gives us slightly better results for fully-convolutional AE than $p = 5$ though learning time is higher. However, we see that for $p = 5$ performance of convolutional AE is much better than for $p = 7$. It can be explained by layer flattening when passing from convolutional layers to linear.

Table 2. Algorithm performance based on patch size p for images taken in 2004 and 2005 years.

Methods	$p \times p$	Classification performance			
		Precision	Recall	Kappa	Time ^a , min
Fully-Conv.	3×3	0.69	0.73	0.70	11+10
	5×5	0.67	0.78	0.70	14+12
	7×7	0.69	0.78	0.72	19+16
Conv.	3×3	0.67	0.74	0.69	12+11
	5×5	0.68	0.79	0.71	17+16
	7×7	0.61	0.81	0.69	24+22

^aPre-training+fine-tuning.

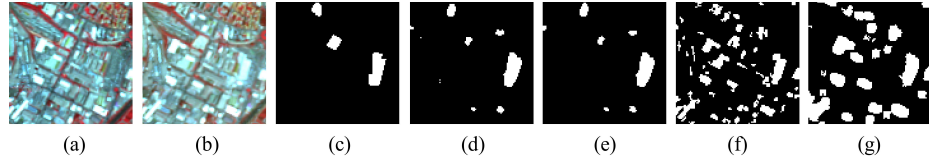


Fig. 3. Classification results. Image extract 100×100 pixels. Example of luminosity sensitivity. a- image taken on May 2004, b - image taken on April 2005, c- ground truth, d- fully-convolutional AE, e- convolutional AE, f- RBM, g- improved RBM.

Some change detection results are presented on Figures 3, 4, 5, 6, 7. All the images are represented in false colors, where red corresponds to vegetation and green to empty fields.

Figure 3 features changes in an urban area: several buildings were constructed (or started to be constructed). The images extracts have great change in luminosity between the two dates. We observe that both convolutional and fully-convolutional AEs have low ratio of false positive changes while the RBM sensitivity in urban area claimed by its authors is confirmed. At the same time, the improved RBM method has less false positives changes than the initial one. This can also be seen in Figures 4 and 6.

Figure 4 shows the construction of a new road. The road limits were correctly identified by all the models, except for the improved RBM model that did not detect the narrow part of the road.

Figure 5 displays changes in an agricultural area between May 2004 and April 2005. The overall seasonal change tendency is the following: the vegetation is more dense in May, the empty fields and fields with young crops have different minor changes between the two images. All the models except improved RBM showed relatively high ratio of false positive changes in vegetation. Nevertheless, the improved RBM missed more changes than other algorithms. The high ratio of false positives changes detected by first three architectures can be explained by the fact that vegetation density might be irregular and it is considered by

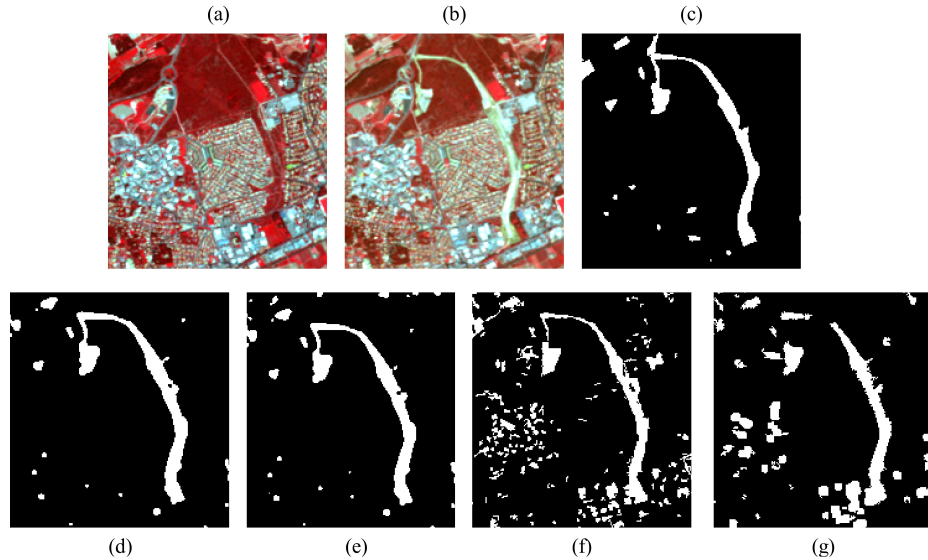


Fig. 4. Classification results. Image extract 180×190 pixels. a- image taken on May 2004, b - image taken on April 2005, c- ground truth, d- fully-convolutional AE, e- convolutional AE, f- RBM, g- improved RBM.

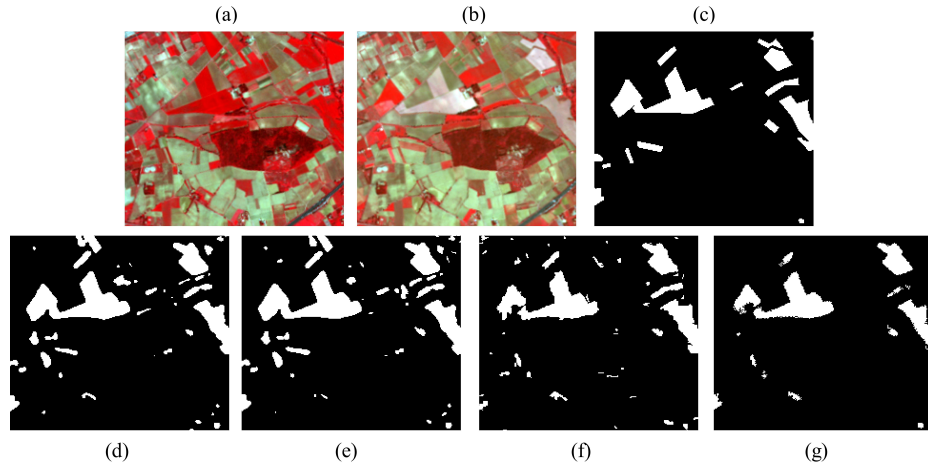


Fig. 5. Classification results. Image extract 230×200 pixels. a- image taken on May 2004, b - image taken on April 2005, c- ground truth, d- fully-convolutional AE, e- convolutional AE, f- RBM, g- improved RBM.

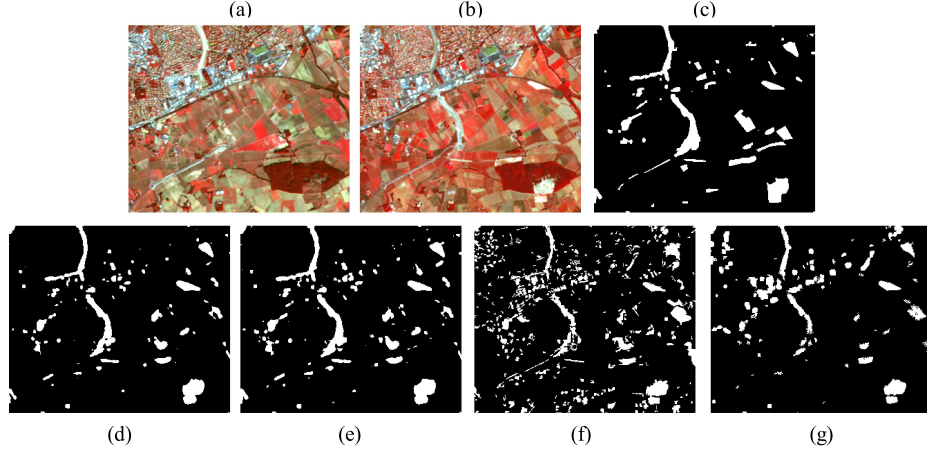


Fig. 6. Classification results. Image extract 320×270 pixels. a- image taken on February 2006, b - image taken on August 2008, c- ground truth, d- fully-convolutional AE, e- convolutional AE, f- RBM, g- improved RBM.

the algorithm as changes. We observe that convolutional AE have slightly better results than other models.

Figure 6 represents changes in an agricultural area between February 2006 and August 2008 as well as some constructions. The overall seasonal change tendency is the following: the fields that are empty in February have vegetation in August, and vice versa. Forest's vegetation state (bottom right corner) has some minor changes. We can see again that the convolutional AE has slightly better results than the fully-convolutional AE. However, the ratio of false positive changes is elevated. Moreover, in most cases, only a part of a field is incorrectly labeled as change. As in the previous example, it can be explained by irregular vegetation density, and further morphological analysis might be needed to obtain better results. At the same time, the initial RBM model showed better performance for the detection of a linear object that corresponds to constructions at the roadside at the lower left part of the image, though the level of false positive changes is high both in urban and agricultural areas.

Figure 7 shows the limitations of the proposed approach for the detection of the construction of a tramway line. Our method have poor quality of change detection for linear objects that can be explained by the patch-wise learning. As a patch reconstruction error determines the change class of its central pixel, changes in 1-2 pixel width linear objects can not be properly detected.

The different approaches performances are presented in Table 3. The algorithms were tested on NVIDIA Titan X GPU with 12 GB of RAM. Based on the presented results and on the performance estimators, we can conclude that joint convolutional AEs slightly outperformed fully-convolutional ones, though the training time stays higher as the model is more complicated. The perfor-

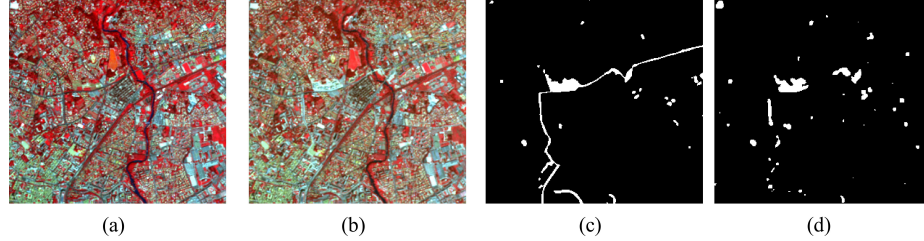


Fig. 7. Classification results. Algorithm limitations. Image extract 300×280 pixels. a- image taken on May 2004, b- image taken on April 2005, c- ground truth, d- convolutional AE.

Table 3. Performance of change detection algorithms on SPOT-5 images.

Methods	Classification performance			
	Precision	Recall	Kappa	Time ^a , min
2004	RBM AE	0.48	0.64	0.52
	Impr. RBM AE	0.52	0.63	0.54
	Conv. AE	0.68	0.79	0.71
	Fully-Conv. AE	0.67	0.78	0.70
2005	RBM AE	0.40	0.61	0.43
	Impr. RBM AE	0.50	0.54	0.48
	Conv. AE	0.76	0.79	0.75
	Fully-Conv. AE	0.80	0.71	0.73
^a Pre-training+fine-tuning.				

mance of joint convolutional AEs can be explained by the higher complexity of the convolutional model. At the same time, both models of our approach showed better performances for change detection than the RBM-based models. However, it can be noted that the initial RBM method still has a high recall and the best training time despite a high level of false positive changes in urban areas compared to our approaches. We can equally conclude that methods with pixel-wise extracted patches have higher performance than initial RBM method where patches are not overlapped. Nevertheless, the improved RBM method detected less changes than the initial RBM method, though the number of false positives changes is much lower and overall classification performance characterized by kappa is higher.

5 Conclusion

In this paper, we have presented unsupervised deterministic approaches for change detection in open source SITS based on AE models. Our experiments have shown that our deterministic AE models perform better than state of the art RBM approaches on a large area with various land cover occupation. Among our

proposed architectures, the joint fully-convolutional AEs model showed slightly better performances in spite of a longer training time.

In future works, we will focus on developing an algorithm for clustering these changes. Furthermore, we will improve our model by adding the analysis of morphological features, leading to more robust results for images with higher variance of seasonal changes.

References

1. Cao, G., Wang, B., Xavier, H., Yang, D., Southworth, J.: A new difference image creation method based on deep neural networks for change detection in remote-sensing images. *International Journal of Remote Sensing* **38**(23), 7161–7175 (2017)
2. Caye Daudt, R., Le Saux, B., Boulch, A., Gousseau, Y.: Urban change detection for multispectral earth observation using convolutional neural networks. *CoRR abs/1810.08468* (2018)
3. Cohen, J.: A coefficient of agreement for nominal scales. *Educational and Psychological Measurement* **20**(1), 37–46 (1960)
4. Cui, W., Zhou, Q.: Application of a hybrid model based on a convolutional auto-encoder and convolutional neural network in object-oriented remote sensing classification. *Algorithms* **11**, 9 (01 2018)
5. Deng, J.S., Wang, K., Deng, Y.H., Qi, G.J.: PCAbased landuse change detection and analysis using multitemporal and multisensor satellite data. *International Journal of Remote Sensing* **29**(16), 4823–4838 (2008)
6. Du, P., Liu, S., Gamba, P., Tan, K., Xia, J.: Fusion of difference images for change detection over urban areas. *IEEE Journal of Selected Topics in Applied Earth Observations and Remote Sensing* **5**(4), 1076–1086 (Aug 2012)
7. El Hajj, M., Bégué, A., Lafrance, B., Hagolle, O., Dedieu, G., Rumeau, M.: Relative radiometric normalization and atmospheric correction of a spot 5 time series. *Sensors* **8**(4), 2774–2791 (2008)
8. Guo, X., Liu, X., Zhu, E., Yin, J.: Deep clustering with convolutional autoencoders. In: Liu, D., Xie, S., Li, Y., Zhao, D., El-Alfy, E.S.M. (eds.) *Neural Information Processing*. pp. 373–382. Springer International Publishing, Cham (2017)
9. Hinton, G.E., Salakhutdinov, R.R.: Reducing the dimensionality of data with neural networks. *Science* **313**(5786), 504–507 (2006)
10. Nielsen, A.A.: The regularized iteratively reweighted MAD method for change detection in multi- and hyperspectral data. *IEEE Transactions on Image Processing* **16**(2), 463–478 (Feb 2007)
11. Otsu, N.: A threshold selection method from gray-level histograms. *IEEE Transactions on Systems, Man, and Cybernetics* **9**(1), 62–66 (Jan 1979)
12. Sublime, J., Troya-Galvis, A., Puissant, A.: Multi-scale analysis of very high resolution satellite images using unsupervised techniques. *Remote Sensing* **9**(5), 495 (2017)
13. Tan, K., Jin, X., Plaza, A., Wang, X., Xiao, L., Du, P.: Automatic change detection in high-resolution remote sensing images by using a multiple classifier system and spectralspatial features. *IEEE Journal of Selected Topics in Applied Earth Observations and Remote Sensing* **9**(8), 3439–3451 (Aug 2016)
14. Xu, Y., Xiang, S., Huo, C., Pan, C.: Change detection based on auto-encoder model for vhr images. *Proc SPIE* **8919**, 02– (10 2013)